Available online at www.sciencedirect.com
ScienceDirect
Trans. Nonferrous Met. Soc. China 31(2021) 2388−2401
Transactions of Nonferrous Metals Society of China
www.tnmsc.cn

Improving sintering kinetics and compositional homogeneity of Inconel 625 superalloy open-cell foams made by suspension impregnation method

Oleg SMORYGO[1], Vitali MIKUTSKI[1], Anastasia VAZHNOVA[1], Viachaslau HANCHAROU[1], Serguei TIKHOV[2], Vinod Kumar JANAGAM[3], Amol Anant GOKHALE[4]

1. O.V. Roman Powder Metallurgy Institute, 41, Platonov str., Minsk 220005, Belarus;
2. Boreskov Institute of Catalysis, Siberian Branch, Russian Academy of Sciences, 5, pr. Lavrentieva, Novosibirsk 630090, Russia;
3. Defence Metallurgical Research Laboratory, Kanchanbagh, Hyderabad 500058, India;
4. Indian Institute of Technology Bombay, Powai, Mumbai 400076, India

Received 7 September 2020; accepted 2 March 2021

Abstract: Open-cell Inconel 625 superalloy foams were prepared by suspension impregnation method which involves replication of pure nickel foam ligaments with a mixed powder suspension and subsequent heat treatments. The objective of the present study is to find a suitable method ensuring complete densification of the superalloy foam ligaments without using low-melting additives and achieving uniform chemical composition at moderate sintering temperatures. Foams prepared using the above methodology were evaluated for the microstructure and compositional variation across the foam ligaments by scanning electron microscopy (SEM) coupled with electron dispersive spectroscopy (EDS). Quasi-static compressive properties of the foams were evaluated. It is shown that if elemental powders of Cr, Mo and Ni are used as additives to the superalloy powder suspension, high ligament density with uniform chemical composition conforming to the Inconel 625 specification is achieved at moderate sintering temperatures. These results are attributed to the formation of low melting eutectics and to acceleration of the diffusion kinetics due to the non-equilibrium thermodynamic conditions created by large compositional gradients in the presence of elemental powders.

Key words: superalloy foam; suspension replication; sintering; diffusion; microstructure

1 Introduction

Superalloy foams with an open-pore reticulated structure are strong candidates for many high-temperature applications, such as sandwich cores in the active thermal protection systems, components of heat exchangers, solar energy volumetric receivers, liners of aircraft high-speed turbofan rotors, and filters of hot gases [1−6]. A feasible approach to make such foams is the replication of highly-porous stochastic foam templates with the required metallic materials [7]. Ni-based superalloys are attractive foam materials because they demonstrate excellent combination of corrosion resistance and mechanical properties at elevated temperatures [8,9].

Highly-porous reticulated structures with a low relative density can be made by electrolytic deposition of metals onto structural elements (ligaments) of a stochastic polymeric foam, by electroless metal reduction, or by decomposition of carbonyls [7,10−13]. After suitable heat treatments to burn off the polymeric template and to sinter the deposited metal coating, a rigid and highly permeable reticulated structure can be achieved.

Corresponding author: Oleg SMORYGO, E-mail: olegsmorygo@yahoo.com, smorygo@tut.by
DOI: 10.1016/S1003-6326(21)65661-3

However, these methods are commonly limited to foams of pure metals like Ni, Cu, and Fe. Complex composition of the foam, also with strong limitations, can be achieved via layer-wise deposition of the constituent metals followed by homogenizing heat treatment [14].

Open-cell metal foams containing multiple alloying elements can be made by replication of the polymeric foam template with a suspension of metal powder(s) in a suitable proportion followed by multiple compressing the template to distribute the suspension uniformly within the template and to remove excess quantities [15−17]. The powders, suspended in the solvent, coat the ligaments of the polymeric foam. This is followed by drying and heat treatments to burn off the organic matter and sinter the powder particles. The "green" strength of the metallic part of this foam is poor, which makes it prone to collapse after burning out the polymeric template. In addition, the densification of the deposited powder during sintering is accompanied by large linear shrinkage resulting in distortion or cracking, particularly in large samples. A large residual porosity within the ligaments is a common problem of this method.

QUEHEILLALT et al [18] used a reticulated vitreous carbon as the replication template to suppress the shrinkage at sintering and ensure structural stability. Inconel 625 superalloy powder was mixed with Ni−Cr−P braze alloy powder (the latter as a transient liquid phase sintering agent) in the impregnation suspension to improve the degree of sintering and reduce post-sintering porosity. The method uses expensive carbon foam as the template, and the presence of the braze alloy additive lowers the foam's high-temperature properties. In another paper, QUEHEILLALT et al [19] used the electron beam directed vapor deposition (EB-DVD) technique to replicate ligaments of the polymeric foam template directly with Inconel 625 layer. However, additional deposition of a low-melting braze powder was necessary to achieve a non-porous ligament microstructure. In addition, EB-DVD process requires complex and expensive equipment, and the ion flux shading limits the template dimensions.

Stochastic open-cell nickel foams can be considered as viable alternatives to carbon foam templates to produce distortion-free reticulated foams with improved corrosion resistance and good thermo-mechanical properties. CHOE and DUNAND [20] performed pack alloying of nickel foams in the mixture of an alloying metal powder, activator for the metal gas-phase transfer, and inert filler. Heating in an inert atmosphere initiated diffusion of the alloying metal into the foam ligaments, thus ensuring highly-porous Ni−Al and Ni−Cr−Al open-cell foams. A post-deposition homogenizing heat treatment eliminated the concentration gradients. PANG et al [21,22] synthesized Y−Cr and Ce−Cr-coated Ni−Cr−Fe alloy foams using the same approach.

A much simpler process of making nickel base alloy foams starting from commercially available pure nickel foams was presented by WALTHER et al [23]. It comprised coating ligaments of the stochastic nickel foam template with a liquid organic binder, sticking a pre-alloyed powder to the binder, and carrying out heat treatments for debindering, transient liquid phase sintering, and diffusion of alloying components into the nickel foam ligaments. The process was stated to be flexible with respect to the targeted foam composition, of which more than 40 have been developed, but the thickness of the foams was limited to 3 mm.

In our recent work [24], the nickel foam template was replicated by multiple impregnations in commercial Inconel 625 powder aqueous suspension followed by the removal of the excess suspension by centrifuging. This process not only retained the advantages of the process described in Ref. [23] but also allowed tailoring of the applied coating thickness. However, unequal diffusion flux rates of the alloying elements into the nickel foam template and poor densification of the applied powder layer, even at temperatures close to the liquidus point, were revealed. The objective of this study was to eliminate these drawbacks. We describe the effect of the sintering conditions on the densification of the applied powder layer, distribution of various alloying elements within the foam ligaments, and mechanical strength of the resultant superalloy foam. The innovative aspect of the study is the rational use of elemental powders mixed with superalloy powder which facilitates the ligament densification and compositional homogenization at moderate sintering temperatures without disturbing the mechanical integrity of the foam. This frees from the need for low melting

additives and ensures effective densification and conversion of pure Ni ligaments into IN625 superalloy ligaments. Moreover, we explain the mechanism of achieving the desired densification and homogenization at moderate sintering temperatures based on the formation of low melting eutectics and creation of sharp initial compositional gradients made possible by the elemental powder addition. Evidently, the approach can be extended to foams based on other alloys as well.

2 Experimental

2.1 Preparation of nickel foam template

Open-cell nickel foams were made in the form of plates with dimensions of 100 mm × 100 mm × 20 mm and the density of (0.17±0.02) g/cm^3 by electrolytic replication of reticulated polyurethane foam with a nominal cell size of 10 ppi. The process for the nickel layer deposition and the composition of the electrolyte are explained in detail in Ref. [25]. The nickel foam plates were sintered in the cracked ammonia atmosphere at 1100 °C for 1 h. Then, samples with a diameter of 30 mm were cut from the plates.

2.2 Preparation of suspensions

Suspensions of metal powder mixtures were prepared in 6% PVA aqueous solution (Celvol 325, Sekisui). The solid phase in the suspension comprised Inconel 625 superalloy powder (IN625, Hoganas) as the main component and elemental Mo, Cr and Ni powders (of Russian origins) in different contents. The contents (in wt.%) of the powder mixtures deposited on the nickel foam (NF) template ligaments and their designations are given in Table 1. The IN625 powder, according to the supplier's data, contained (in wt.%): 21.40 Cr, 8.90 Mo, 3.62 Nb, 0.58 Fe, 0.38 Mn, 0.43% Si, 0.01 C, 0.01 Al, 0.01 Ti and balance Ni. The particle size distribution was: d_{10}=23.1 μm, d_{50}=38.2 μm, and d_{90}=59.8 μm. The elemental powders were of technical grade purity and the following average particle sizes d_{50}: 10.9 μm (Mo), 20.4 μm (Cr), and 13.5 μm (Ni). SEM images of the powders used in this research are presented in Fig. 1. Different contents of metal powders, as given in Table 1, were mixed in the PVA aqueous solution in a glass vessel for 30 min using a propeller stirrer. The solid content in the suspension was 87 wt.% in all cases.

Table 1 Contents of powder mixtures used for replication of nickel foam (NF) template

No.	Designation of sample type	Powder content in mixture/wt.%			
		IN625	Ni	Cr	Mo
1	NF/625	100	−	−	−
2	NF/625−2.5Ni−2.5Cr	95	2.5	2.5	−
3	NF/625−2Ni−2Cr−1Mo	95	2	2	1
4	NF/625−1Ni−9Cr	90	1	9	−
5	NF/625−1Ni−10Cr−4Mo	85	1	10	4
6	NF/625−10Cr−5Mo	85	−	10	5

2.3 Preparation of superalloy foams

The nickel foam templates were impregnated with the mixed powder suspensions described above, centrifuged at the overload of 12 g to remove the excess suspension, and dried above 100 °C. Three successive impregnation−centrifuging−drying cycles were required to achieve the foam density of 0.7−0.8 g/cm^3 corresponding to the fractional porosity range of ~0.90−0.92. Nickel foam ligaments were uniformly coated with the powder layers throughout the template without disturbing significantly their open-cell structure. Finally, the foam samples were put in graphite containers and heated in vacuum (<10^{-3} Pa) to sinter the powder layers and enable inter-diffusion of the alloying elements between the various powders and the pure Ni ligaments of the template. In all cases, the sintering was carried out for 2 h at different temperatures in the range of 1290−1335 °C.

2.4 Characterization methods

SEM images of the foams were obtained using the scanning electron microscope (Mira, Tescan). Chemical analyses at different locations along the foam ligament thickness were carried out with an energy-dispersive EDX spectrometer (INCA−350, Oxford Instruments). To quantify the local compositional deviations from the average values at different locations within the ligaments, average contents of Cr, Mo and Nb were firstly determined. Thereafter, local compositions were measured at 3−5 points in the nickel foam template area. The deviation in the composition from the average value was calculated as the ratio of the local elemental concentration to its average

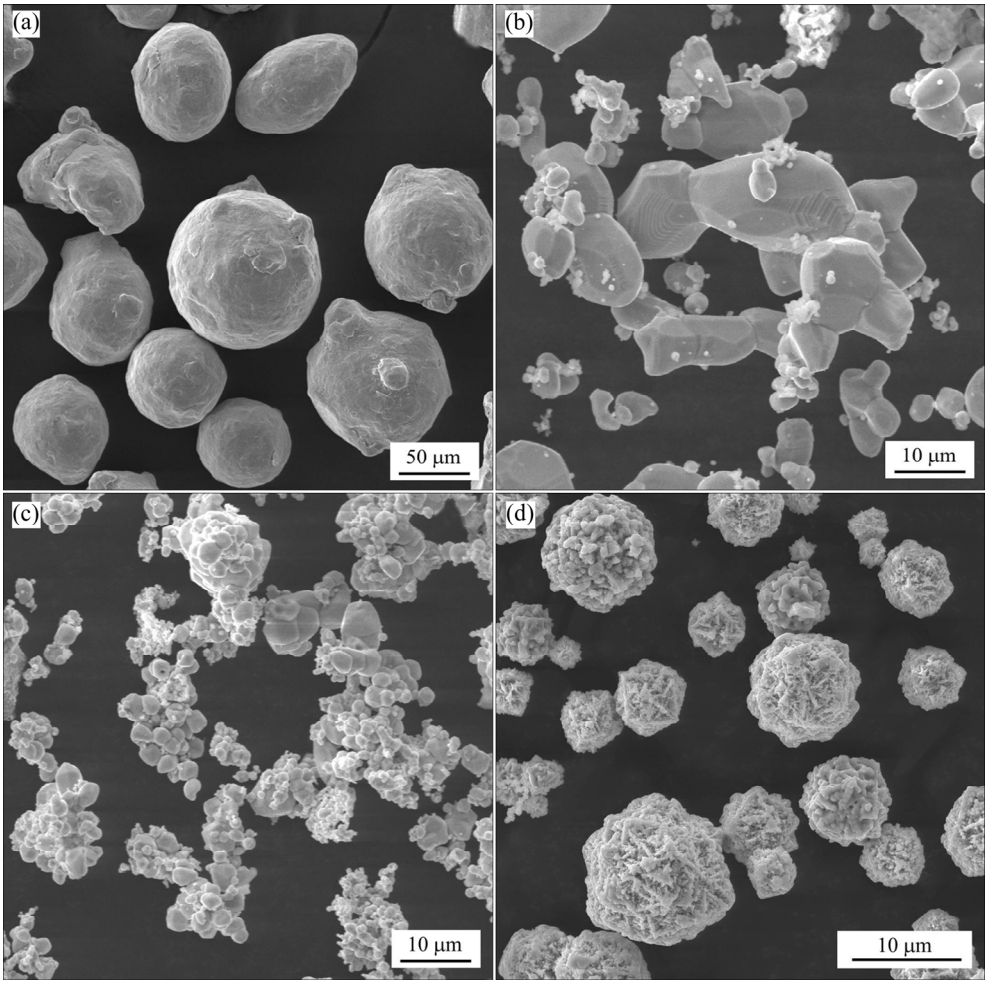

Fig. 1 SEM images of powders used for preparation of superalloy foams: (a) IN625; (b) Cr; (c) Mo; (d) Ni

concentration. Metallographic samples were etched with Marble's reagent for 1 min to reveal the microstructure. Mechanical strength of the foams was evaluated using a testing machine (H150KU, Tinius Olsen) under monotonic compression at the crosshead speed of 2 mm/min with the accuracy of ±5 N, which was less than 1% of typical onset and plateau loadings. At least 6 samples of each type were characterized.

3 Results and discussion

3.1 Theoretical basis for processing scheme and selection of raw materials

The powder layers applied over the nickel foam ligaments by the impregnation method described above have no chance to be compacted as those in standard powder metallurgy components. This creates problems for further densification during sintering and homogenization of the chemical composition by solid state diffusion. Here, two mechanisms were aimed to drive the densification and homogenization processes: (1) liquid phase sintering; (2) faster diffusion kinetics due to the creation of non-equilibrium thermodynamic conditions by introducing the elemental powders in addition to the master alloy powders.

In a general case, the kinetics and degree of sintering depend on several factors such as powder particle size, degree of powder compaction and temperature. To reduce the sintering time typical for solid state sintering, additives which produce low melting phase(s) are used, which results in "liquid phase sintering". The liquid phase may be sustained till the end of sintering, remaining as the "matrix" phase in a composite-like microstructure, or may be transient due to the homogenization of the chemical composition, resulting in a nearly single phase microstructure at the sintering temperature [26]. If

there is good wetting between the liquid and the solid phases, the liquid penetrates between the powder particles and facilitates sintering mechanisms such as powder particle rearrangement, solid dissolution and re-precipitation. Besides, elemental diffusion through the liquid state is a few orders of magnitude faster than that in the solid state which accelerates sintering kinetics. In the present case, 625 superalloy powders, the elemental powders, and the pure Ni ligaments together form an interacting system in which large solubility exists for the alloying elements Cr, Mo and Nb in a common parent element Ni. For example, 47 wt.% Cr dissolves in Ni at the eutectic temperature of 1345 °C [27], 47.7 wt.% Mo dissolves in Ni at the eutectic temperature of 1310 °C [28] and 18.9 wt.% Nb dissolves in Ni at approximately 1275 °C [29]. Processing of powder blends, consisting of powder feedstock produced by mixing distinct elemental powdered components, can promote more intensive densification and diffusion than processing of pre-alloyed powders. Due to the presence of particles with different compositions in the powder mixture, reactions between several different phases or components can occur simultaneously at sintering. The direction of the processes is towards thermodynamic equilibrium in the system [30]. In the present case, the idea is to mix the master alloy powders with elemental powders to form the desired superalloy across the in-situ foam ligaments during sintering via diffusion homogenization. The presence of elemental powders (Cr and Mo) promotes large compositional gradients which can play an important role in reaching the equilibrium composition through intense diffusive fluxes, in comparison with those using alloy powders. Nb was not added in the elemental form, since it has the potential to form undesired Laves phases [31].

3.2 Densification of deposited powder layer

The effect of sintering temperature on densification of the powder layer deposited on the nickel foam ligaments is explained in Table 2.

The evolution of densification of the foam ligaments with increasing sintering temperature in the case of IN625 powder deposition (NF/625 sample) is illustrated in Fig. 2. The sintering temperatures presented here are to be considered in the light of the solidus and the liquid temperatures of the IN625 alloy, which are 1290 and 1350 °C, respectively [32]. As can be seen, no remarkable densification was found after sintering at 1290 and 1305 °C: the boundary between the NF template surface and the highly-porous powder layer could be distinguished, and only small necks are seen to have formed between the contacting powder particles (Figs. 2(a, b)). At 1320 °C, coalescence of pores and remarkable densification of the powder layer occurred. However, the residual porosity was too high (Fig. 2(c)). At a still higher sintering temperature of 1335 °C, almost complete densification was observed, and the interface between the Ni ligaments of the foam template and the deposited powder layer disappeared (Fig. 2(d)). However, a small amount of porosity in the form of large isolated pores still existed. Sintering at higher temperatures approaching the superalloy liquidus temperature of ~1350 °C resulted in complete sample melting, which is not desired. In summary, sintering close to the liquidus temperature of IN625 was required to obtain good sintered density if only IN625 powder was deposited.

Such a densification behavior, of which densification is insignificant at lower sintering temperatures and increases sharply close to the liquidus temperature, is very different from that reported for typical powder metallurgy processes,

Table 2 Effect of sintering temperature on densification of deposited powder layer

No.	Sample type	Sintering temperature/°C			
		1290	1305	1320	1335
1	NF/625	No densification	No densification	Large residual porosity	Densely sintered
2	NF/625−2.5Ni−2.5Cr	−	Large residual porosity	Small residual porosity	Densely sintered
3	NF/625−2Ni−2Cr−1Mo	−	Large residual porosity	Densely sintered	Densely sintered
4	NF/625−1Ni−9Cr	−	Large residual porosity	Densely sintered	Buckling, surface fusion
5	NF/625−1Ni−10Cr−4Mo	Densely sintered	Densely sintered	Buckling, surface fusion	−
6	NF/625−10Cr−5Mo	Densely sintered	Densely sintered	Buckling, surface fusion	−

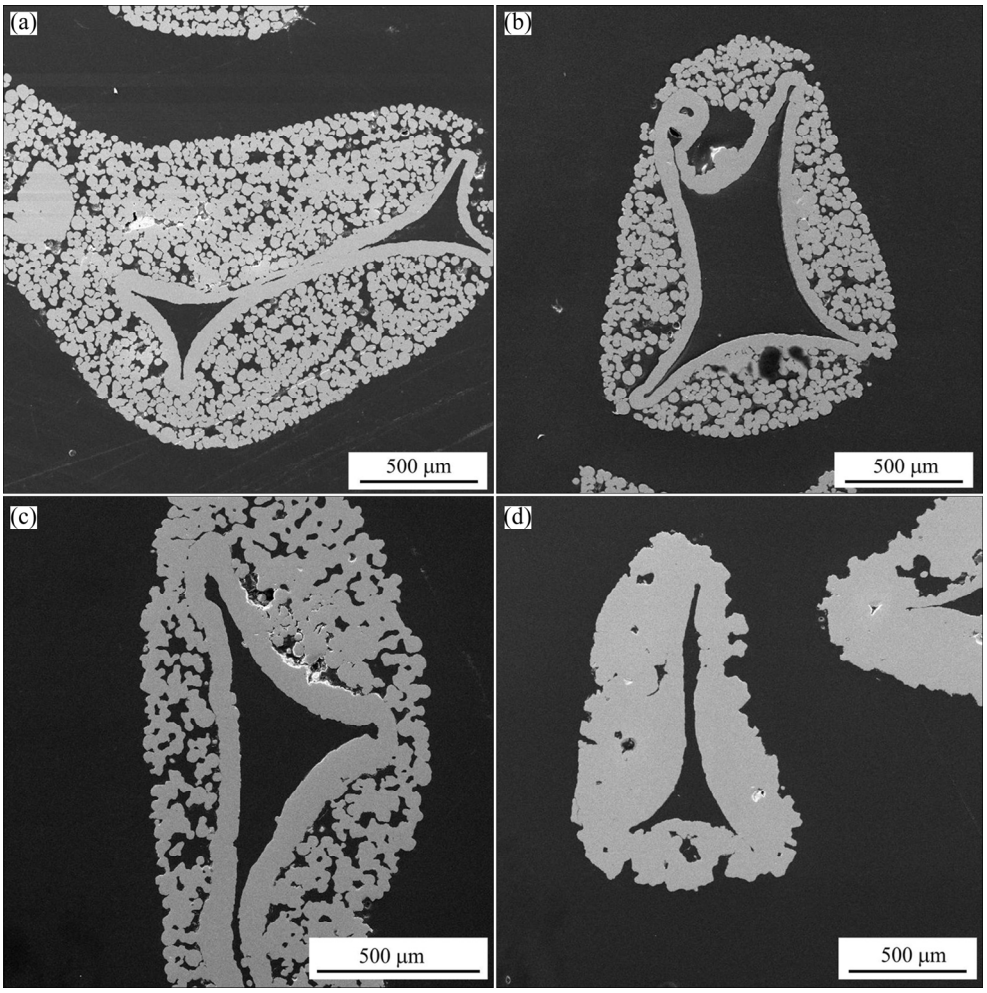

Fig. 2 SEM images showing ligament cross-sections of NF/625 foams depending on sintering temperature: (a) 1290 °C; (b) 1305 °C; (c) 1320 °C; (d) 1335 °C

where gradual and uniform elimination of the residual porosity with increasing sintering temperature is seen and, that too, at lower sintering temperatures. MOSTAFAEI et al [33] prepared samples by powder bed binder jet printing of IN625 superalloy powders with the average particle size of 31.8 μm. A very high level of relative density of 99.6% was obtained after sintering at 1290 °C (i.e. below the solidus temperature). ÖZGÜN et al [34] sintered injection molded IN625 superalloy powders with the average particle size of 11.1 μm. A high relative density of 98% was attained after sintering at 1300 °C (i.e. slightly above the solidus temperature). UNVER et al [35] used the same IN625 powders to make superalloy foam by the powder space-holder technique at the uniaxial compacting pressure of 150 MPa. Vacuum sintering at 1300 °C also ensured a high relative density of 97%. The main difference between the above three processes on one hand and suspension impregnation process on the other hand is that the green densities achievable in suspension impregnation are lower, which might have necessitated sintering at higher temperatures to achieve a comparable level of densification.

Figure 3 presents higher magnification views of the powder layers after sintering at 1305 °C and compares Samples 1, 3, and 4 concerning the state of powder agglomeration, size and distribution of porosity (Figs. 3(a, c, d)). In the as-deposited condition, the powder particles are loosely held in the form of unevenly distributed small aggregates (not shown). Sintering of Sample 1 at 1305 °C led to partial coagulation of the powder aggregates (Fig. 3(a)). After sintering at a higher temperature of 1320 °C, the primary porous structure consisting of particles smaller than 50 μm had transformed into a secondary porous structure consisting of large

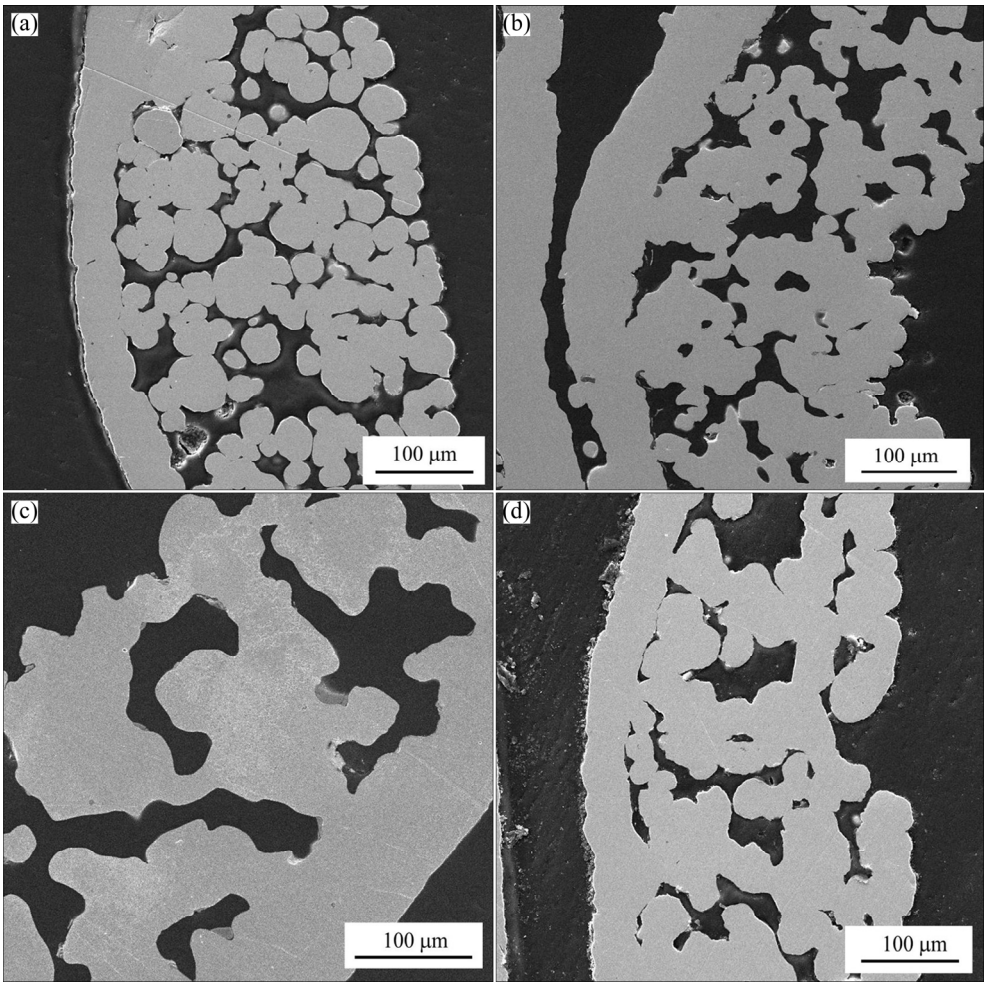

Fig. 3 SEM images showing powder layer over NF template ligament: (a) NF/625 foam, 1305 °C; (b) NF/625 foam, 1320 °C; (c) NF/625−1Ni−9Cr, 1305 °C; (d) NF/625−2Ni−2Cr−1Mo, 1305 °C

densely sintered clusters of 100−200 μm size with large pores (Fig. 3(b)). In Sample 3 (NF/625−1Ni−9Cr) and Sample 4 (NF/625−2Ni−2Cr−1Mo) that had the elemental powder additives and were sintered at 1305 °C, the agglomeration of the powders and the coarsening of the porosity had progressed more as compared to Sample 1 (NF/625) sintered at either 1305 or 1320 °C. This resulted in concentrated porosity and fewer but larger agglomerates without any powdery appearance (Figs. 3(c, d)). This clearly shows the beneficial effect of elemental powder additions on reducing the sintering temperature for comparable progress of sintering. Further densification of the deposited layer was only possible at higher sintering temperatures where significant fusion occurred.

A comparison of the sintering behavior of all the samples at different temperatures showed that introducing elemental powder additives to IN625 powder resulted in: (1) the decrease in sintering temperatures by 15−45 °C, approaching values as low as the superalloy solidus temperature (~1290 °C) to achieve a high level of densification; (2) a wider allowable temperature range for complete densification. In blends containing elemental molybdenum powder, the beneficial effect on densification was more pronounced, which is presumed to be due to the formation of Ni−Mo eutectic liquid in the inter-particle region.

Figure 4 presents SEM images of the ligaments and their cross-sections of foams prepared using the elemental powder additives (in addition to IN625), which were sintered under conditions that gave the highest levels of densification. As shown in Fig. 4, complete densification of the ligaments without any residual porosity was achieved in all the cases, and the densification temperature range shifted to lower temperatures with increasing content of the powder

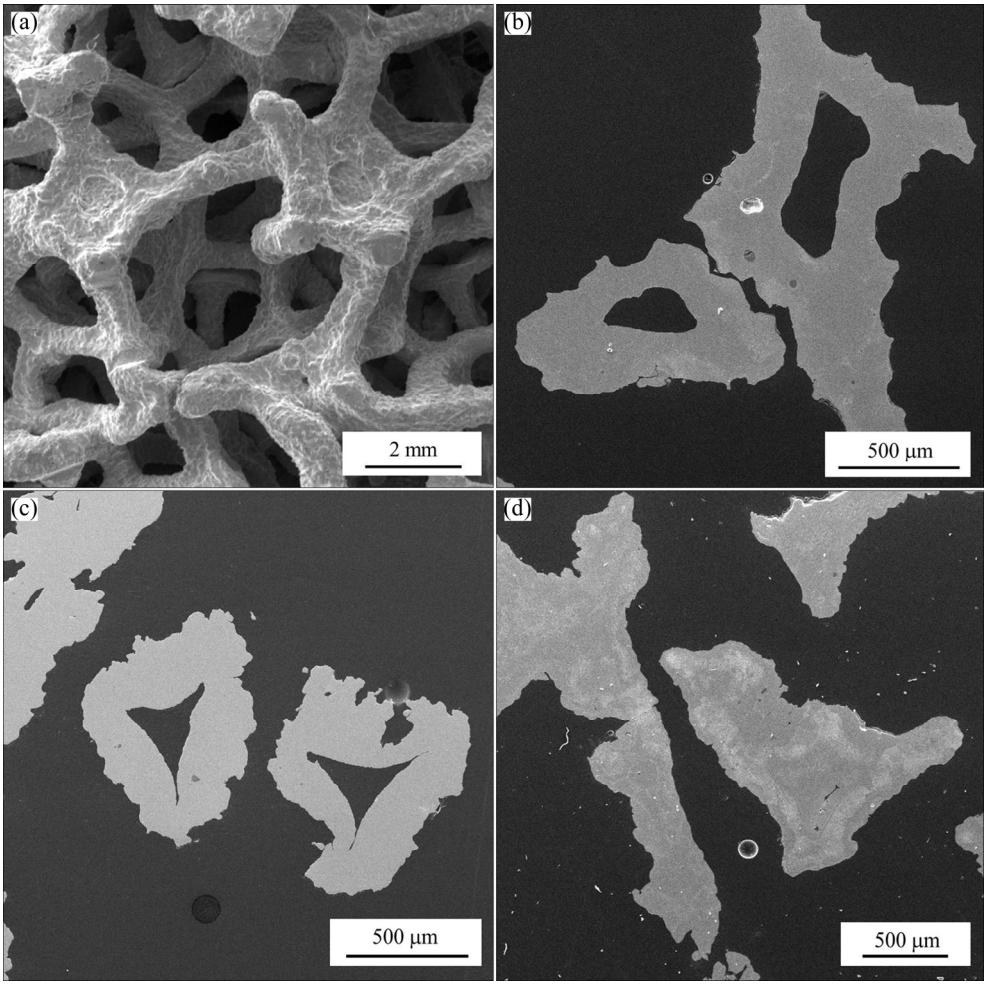

Fig. 4 SEM images showing foam structure (a) and cross-sections of densely sintered ligaments (b−d) in different foam types: (a) NF/625−10Cr−5Mo, 1305 °C; (b) NF/625−2Ni−2Cr−1Mo, 1335 °C; (c) NF/625−1Ni−9Cr, 1320 °C; (d) NF/625−1Ni−10Cr−4Mo), 1305 °C

additives. The larger quantities of additives present in Sample 5 (NF/625−1Ni−10Cr−4Mo) and Sample 6 (NF/625−10Cr−5Mo) led to the collapse of the internal channels of the foam ligaments during sintering at 1305 °C. This indicates the occurrence of partial liquation during sintering within the NF template area since significant diffusion into the dense nickel ligaments can only be expected under liquid phase sintering. At the same time, it can be seen in the image of Fig. 4(a) that the original cellular structure of the foams remains unchanged.

3.3 Degree of homogenization

As can be seen in the images in Figs. 2 and 3, two distinct areas within the foam ligaments are present: (1) the NF template area and (2) the sintered powder layer with residual porosity, the level of which depends on the layer composition and the sintering temperature. In the as-suspension-deposited condition, the foam structure consists of the tubular Ni ligaments with the wall thickness of 20−30 μm and the mixed powder deposit which coats the Ni ligaments. The sintering treatment not only causes the densification of the powder layer but also initiates diffusion-aided homogenization of the composition. The kinetics of sintering depends on factors such as temperature, the diffusivity of the alloying elements, the volume fraction of the liquid phase, and the boundary area between the layers.

The level of homogenization in the NF ligaments after sintering at different temperatures, expressed in terms of the actual alloy content within the Ni ligament as its average composition, is illustrated in Fig. 5 for different powder mixtures used. The degree of homogenization is seen to be

strongly dependent on the sintering temperature. It is evident that if the sintering temperature is below the 625 alloy solidus temperature (solid-state sintering), the degree of homogenization is low. However, when the sintering temperature increases within the liquidus−solidus temperature range, greater compositional uniformity is achieved via liquid phase sintering. Also, the use of elemental powders is expected to facilitate the formation of low melting eutectic liquids of the corresponding binary systems.

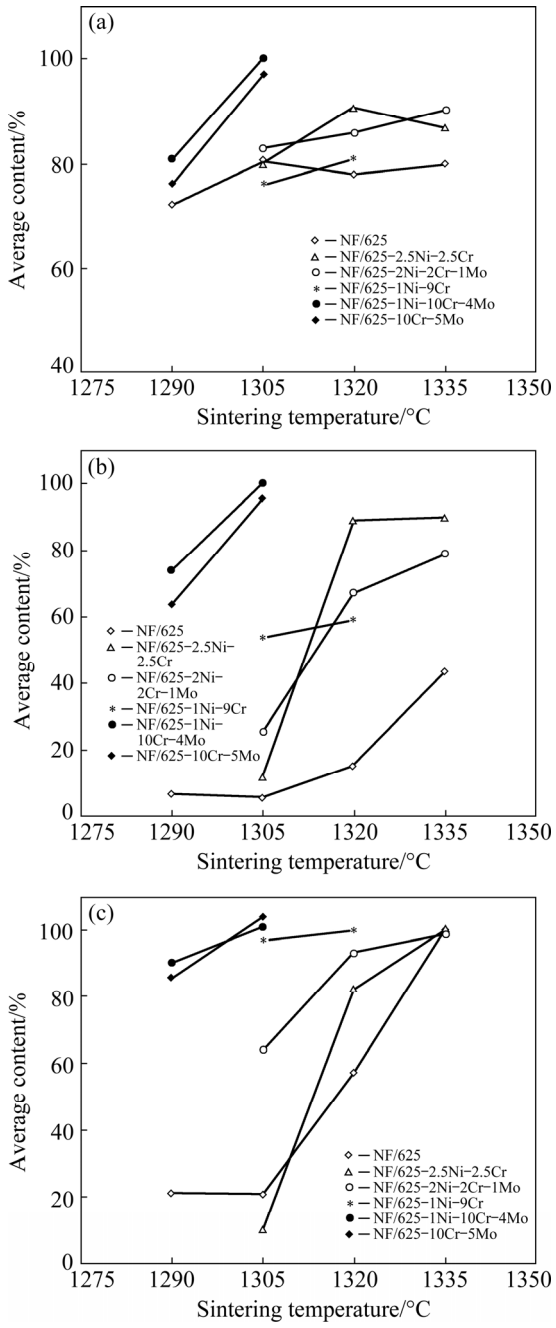

Fig. 5 Average contents of alloying elements in NF area as compared to their average contents in foam: (a) Cr; (b) Mo; (c) Nb

The homogenization kinetics is seen to be the fastest for Nb, intermediate for Cr, and the slowest for Mo for all the powder mixtures (Fig. 5). HARGATHER et al [36] estimated the pre-exponential factors and the activation energies for 26 elements in dilute solutions of FCC nickel. In particular, the values of the diffusion parameters at two different temperatures of 700 K (427 °C) and 1700 K (1427 °C) were given. Based on these data, diffusion coefficients of Cr, Mo, and Nb at 1300 °C have been calculated and presented in Table 3. The self-diffusion coefficient D_0 and activation energy at 1427 °C (near the sintering temperature) from Ref. [36] have been used.

Table 3 Diffusion coefficients of Cr, Mo and Nb (as dilute solutions) in Ni at 1300 °C

Element	D_0/(m^2·s^{-1})	Activation energy per atom/eV	Diffusion coefficient/(m^2·s^{-1})
Cr	9.25×10^{-5}	3.11	9.59×10^{-15}
Mo	1.09×10^{-5}	2.90	5.34×10^{-15}
Nb	6.33×10^{-5}	2.74	1.01×10^{-13}

Table 3 shows that the diffusion coefficient of Nb is at least an order of magnitude higher than that for Cr, which in turn, is somewhat higher than that of Mo. This explains the relative kinetics of the homogenization of the elements during sintering. A uniform distribution of Cr and Mo is observed in two of the foam types (NF/625−1Ni−10Cr−4Mo and NF/625−10Cr−5Mo), which have the highest aggregate solute contents and are expected to form the greatest amount of liquid during sintering. When the sintering temperature exceeds the IN625 superalloy solidus temperature, the sintering kinetics will be accelerated further, since the NF ligaments which are initially below the freezing temperature are increasingly brought into the two-phase temperature range, further promoting liquid phase sintering.

3.4 Microstructures of sintered and homogenized foams

Past researches on IN625 superalloy powder metallurgy products after the solid-state or liquid-phase sintering showed that their microstructures consisted of round grains with the grain-boundary as well as intra-granular precipitates, which were

either niobium carbides or metallic phases enriched in Nb and Mo [33,34].

A typical microstructure of the foams made in the present work in the best-homogenized condition is presented in Fig. 6. The microstructure is typical of as-cast 625 superalloy showing round grains with a network of inter-granular precipitate particles. The nature of the microstructure is similar across the entire cross-section of the foam ligaments in two types of foams (NF/625−1Ni−10Cr−4Mo and NF/625−10Cr−5Mo), strongly suggesting that liquation occurred in the base nickel foam template as well as in the powder deposit. Liquation within the nickel foam template area, despite the sintering temperature being below the melting point of pure nickel, is attributed to the diffusion of the alloying elements bringing down the solidus temperature below the sintering temperature.

Detailed information about the melting and solidification mechanisms of 625 alloys can be found in Refs. [37,38]. It was demonstrated in Refs. [37,38] that the principal feature of the solidification process in 625 cast alloys is the enrichment of Nb in the last liquid before complete solidification. As a result, the characteristic solidification phases formed are as follows: FCC γ-Ni solid solution; MC and/or MC_6 type niobium carbides; eutectic-like Laves phases enriched in Nb and Mo. The Laves phases are topologically close-packed A_2B type intermetallic compounds in which, in the case of 625 superalloy, Positions A in the lattice can be occupied by Cr and Ni, whereas heavy elements (Nb and Mo) occupy Positions B. The solidification path and the final microstructure of 625 superalloys are strongly influenced by the real content of alloying elements and the levels of minor impurities. The alloy powders used in the present work contained a very low amount of carbon. Besides, since Nb was not introduced as elemental powder, its content in the final foam approached the lower possible limit. Thus, the formation of carbides was limited to separate micron-scale inclusions (Fig. 6(b)) [37], although their exact stoichiometry (MC or MC_6 type) was not determined. EDS elemental analysis revealed that the grain boundaries were significantly enriched in Nb and Mo as compared to the average foam composition, suggesting the formation of the Laves phase precipitates. The Laves phases are known to have a detrimental effect on the alloy mechanical properties. The presence of the Laves phases may be promoted by Si impurity that was present in the as-supplied superalloy powders to a reasonable level [35].

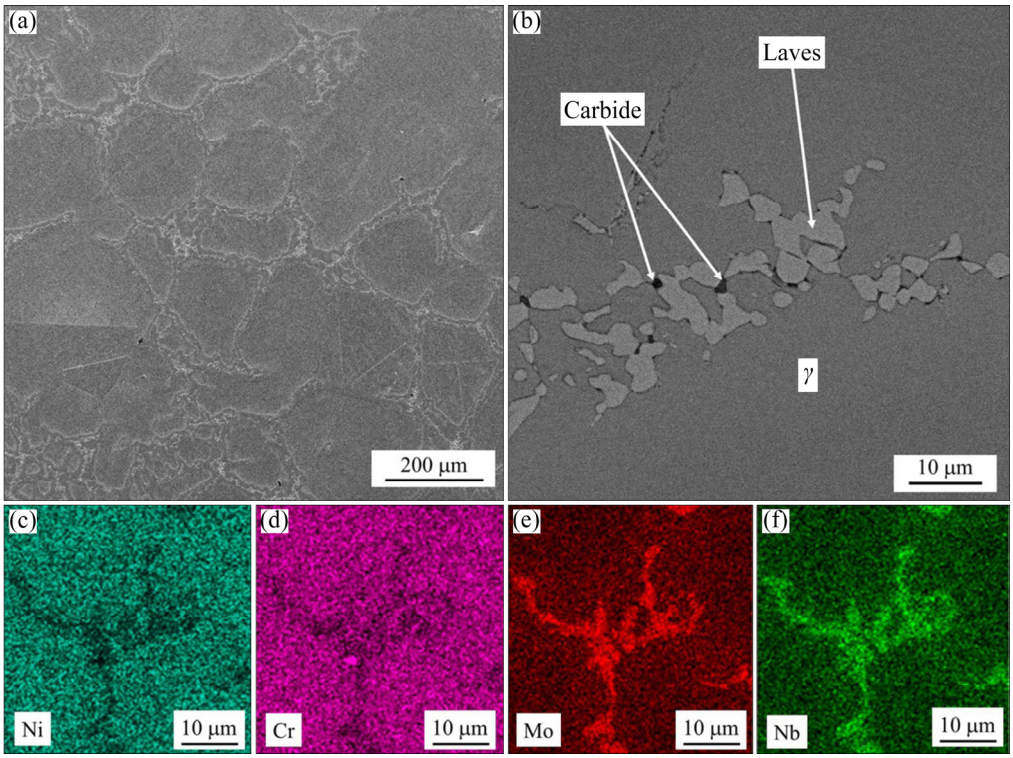

Fig. 6 Microstructures (a, b) and EDX elemental maps in precipitate area (c−f) of NF/625−1Ni−10Cr−4Mo sample sintered at 1305 °C

3.5 Compressive properties of superalloy foams

The quasi-static compression stress−strain curves of the NF/625 foams sintered at different temperatures are demonstrated in Fig. 7. The stress−strain response of foams sintered at lower temperatures, at which the sintering is incomplete (i.e. having large residual porosity), is typical of foams with the ligaments consisting of distinct layers with unequal compositions, residual porosities, and different (brittle and ductile) mechanical behaviors [39]. In such foams, the curves contain clear peak corresponding to the initiation of damage within the brittle component, followed by the post-peak plateau corresponding to the plastic deformation of the load-bearing NF skeleton. When the sintering conditions ensured complete densification of the powder layers (e.g. 1335 °C for NF/625 foams), the stress−strain curves had a classical shape of ductile foams and contained a long plateau [40].

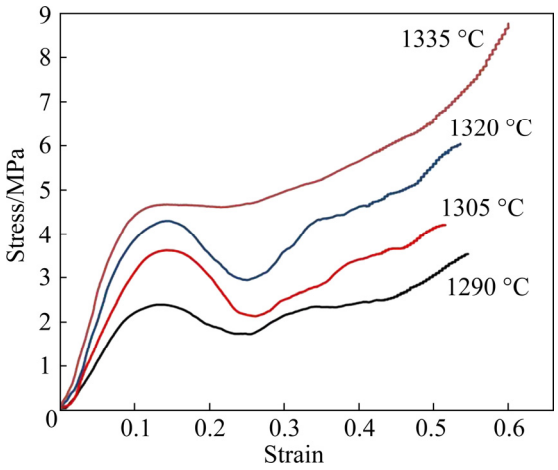

Fig. 7 Stress−strain curves of NF/625 foams sintered at different temperatures

Figure 8 shows the compressive strength dependence on the sintering temperature of different superalloy foams prepared in this research. Here, the strength value corresponds to the peak stress (if it exists), or to the intersection point of the initial loading and the plateau slopes. The graphs display general trends and the data cannot be considered as statistically significant because the samples of the same type had moderate density deviation 0.7−0.8 g/cm^3, while the number of samples was limited to 6−8 pieces of each type, and a large scatter in the measured values of compressive strength was observed. In spite of this, it is clear that the compressive strength increases with the increase in the sintering temperature which, in turn, can be attributed to the improved densification of the deposited powder layer. The effect of the foam composition and the composition uniformity was not statistically reliable; almost all foam samples in which the deposited powder layer was densely sintered had similar average compressive strength values of about 5 MPa. A slightly lower strength of two types of foams (NF/625 and NF/625−2.5Ni−2.5Cr) can be attributed to the minor residual porosity in the form of large isolated pores that were observed after sintering at 1335 °C.

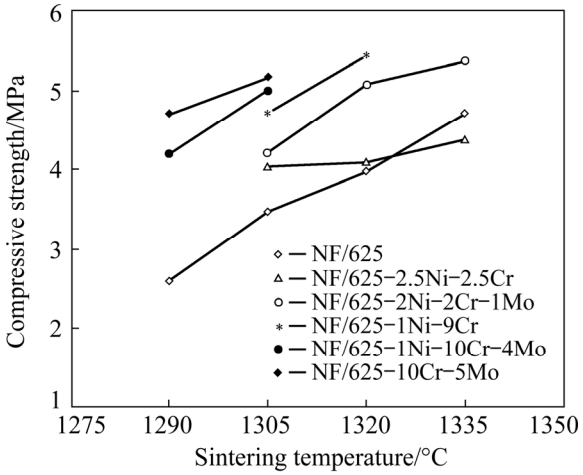

Fig. 8 Compressive strength of different foams depending on sintering temperature

Additional heat treatments which were not explored in this research, such as sequential solution heat treatment, quenching and aging, can lead to a significant increase in the strength of the studied material due to the microstructure evolution [34,41]. At the same time, a simultaneous significant decrease in the fracture toughness should be expected [41,42].

4 Conclusions

(1) Open-cell superalloy foams with a uniform microstructure were made by a simple method comprising replication of a stochastic nickel foam template with commercial Inconel 625 superalloy powders, followed by high-temperature vacuum sintering to densify the applied powder and ensure uniform distribution of alloying elements across the foam ligaments.

(2) Heating the foams to temperatures that

were close to the 625 superalloy liquidus point ensured the densification of the powder layer with low residual porosity but did not ensure fast diffusion of the alloying elements (Mo, Cr and Nb) into the nickel foam template ligaments.

(3) Adding elemental powders (Mo and Cr) to the master alloy powders led to lower densification temperature and more intensive diffusion processes, the latter can be attributed to the initial non-equilibrium conditions in the system with strong composition gradients as well as the local formation of low-temperature eutectic melts in binary systems.

(4) When 5 wt.% of Cr powder and 4−5 wt.% of Mo powder were added to Inconel 625 powder, complete densification of the applied powder mixture occurred, and the composition was uniform across the foam ligaments. The microstructure was similar to that of as-cast 625 superalloy, which included inter-granular Laves phase precipitates and micron-scale carbide inclusions.

(5) The compressive yield strength (~5 MPa at 0.7−0.8 g/cm^3) was found to be dependent on the sintering condition of the applied powder layer and not sensitive to the composition non-uniformity.

Acknowledgments

The authors gratefully acknowledge financial support from DMRL, India (No. 7196-22), Belarusian Republican Foundation for Fundamental Researches (No. T20R-049), and Russian Foundation for basic Research (No. 20-53-00009-Bel).

References

[1] DEVER J A, NATHAL M V, DICARLO J A. Research on high-temperature aerospace materials at NASA Glenn Research Center [J]. Journal of Aerospace Engineering, 2013, 26: 500−514.

[2] RAKOW J F, WAAS A M. Thermal buckling of metal foam sandwich panels for convective thermal protection systems [J]. Journal of Spacecraft and Rockets, 2005, 42: 832−844.

[3] ALBANAKIS C, MISSIRLIS D, MICHAILIDIS N, YAKINTHOS K, GOULAS A, OMAR H, TSIPAS D, GRANIER B. Experimental analysis of the pressure drop and heat transfer through metal foams used as volumetric receivers under concentrated solar radiation [J]. Experimental Thermal and Fluid Science, 2009, 33: 246−252.

[4] SUTLIFF D L, GLENN J H, JONES M G, HARTLEY T C. High-speed turbofan noise reduction using foam-metal liner over-the-rotor [J]. Journal of Aircraft, 2013, 50: 1491−1503.

[5] WANG Xin-zhi, HE Yu-rong, ZHENG Yan, MA Jun-jun, SCHLABERG H I. Analytic estimation and numerical modeling of actively cooled thermal protection systems with nickel alloys [J]. Chinese Journal of Aeronautics, 2014, 27: 1401−1412.

[6] COOKSON E J, FLOYD D E. Application of reticulated metal foam to gas fired infrared burners [J]. High Temperature Materials and Processes, 2007, 26: 269−274.

[7] ASHBY M F, EVANS A G, FLECK N A, GIBSON L J, HUTCHINSON J W, WADLEY H N G. Metal foams: A design guide [M]. Oxford, UK: Butterworth-Heinemann, 2000.

[8] GEDDES B, LEON H, HUANG X. Superalloys: Alloying and performance [M]. Materials Park, OH: ASM International, 2010.

[9] DU Bei-ning, HU Zi-yang, SHENG Li-yuan, CUI Chuan-yong, YANG Jin-xia, ZHENG Yu-feng, SUN Xiao-feng. Tensile, creep behavior and microstructure evolution of an as-cast Ni-based K417G polycrystalline superalloy [J]. Journal of Materials Science and Technology, 2018, 34: 1805−1816.

[10] COLOMBO P, DEGISCHER H P. Highly porous metals and ceramics [J]. Materials Science and Technology, 2010, 26: 1145−1158.

[11] BANHART J. Characterisation and application of cellular metals and metal foams [J]. Progress in Materials Science, 2001, 46: 559−632.

[12] NEIKOV O D. Handbook of non-ferrous metal powders [M]. 2nd ed. Amsterdam: Elsevier, 2019: 323−349.

[13] TIAN Qing-hua, GUO Xue-yi. Electroless copper plating on microcellular polyurethane foam [J]. Transactions of Nonferrous Metals Society of China, 2010, 20(S1): s283−s287.

[14] DUAN D L, LI S, DING X J, JIANG S L. Preparation of Ni−Cr alloy foams by electrodeposition technique [J]. Materials Science and Technology, 2008, 24: 461−466.

[15] HO N S K, LI P F, RAGHAVAN S, LI T. The effect of slurry composition on the microstructure and mechanical properties of open-cell Inconel foams manufactured by the slurry coating technique [J]. Materials Science and Engineering A, 2017, 687: 123−130.

[16] ZHAI W, YU X, SONG X, ANG L Y L, CUI F S, LEE H P, LI T. Microstructure-based experimental and numerical investigations on the sound absorption property of open-cell metallic foams manufactured by a template replication technique [J]. Materials and Design, 2018, 137: 108−116.

[17] QUADBECK P, KÜMMEL K, HAUSER R, STANDKE G, ADLER J, STEPHANI G, KIEBACK B. Structural and material design of open-cell powder metallurgical foams [J]. Advanced Engineering Materials, 2011, 13: 1024−1030.

[18] QUEHEILLALT D T, KATSUMURA Y, WADLEY H N G.

Synthesis of stochastic open cell Ni-based foams [J]. Scripta Materialia, 2004, 50: 313−317.

[19] QUEHEILLALT D T, HASS D D, SYPECK D J, WADLEY H N G. Synthesis of open-cell metal foams by templated directed vapor deposition [J]. Journal of Materials Research, 2001, 16: 1028−1036.

[20] CHOE H, DUNAND D C. Synthesis, structure, and mechanical properties of Ni−Al and Ni−Cr−Al superalloy foams [J]. Acta Materialia, 2004, 52: 1283−1295.

[21] PANG Q, HU Z L, WU G H. Preparation and oxidation performance of Y and Ce-modified Cr coating on open-cell Ni−Cr−Fe alloy foam by the pack cementation [J]. Journal of Materials Engineering and Performance, 2016, 25: 5189−5200.

[22] PANG Qiu, HU Zhi-li, WANG Guo-rong. Effect of Ce content on mechanical properties of Ce/Cr coated open-cell Ni−Cr−Fe alloy foams [J]. Transactions of Nonferrous Metals Society of China, 2017, 27: 1052−1062.

[23] WALTHER G, KLÖDEN B, BÜTTNER T, WEISSGÄRBER T, KIEBACK B, BÖHM A, NAUMANN D, SABERI S, TIMBERG L. A new class of high temperature and corrosion resistant nickel-based open-cell foams [J]. Advanced Engineering Materials, 2008, 10: 803−811.

[24] SMORYGO O, MIKUTSKI V, HANCHAROU V, TARUSOV I, ILYUSHCHANKA A, VINOD KUMAR J, SADYKOV V. Open-cell superalloy foams via the combined electrolytic-suspension route [C]//Proc Euro PM2017 Congress & Exhibition. Chantilly. France: EPMA, 2017: 1−6.

[25] LEONOV A N, SMORYGO O L, SHELEG V K. Monolithic catalyst supports with foam structure [J]. Reaction Kinetics and Catalysis Letters, 1997, 60: 259−267.

[26] GERMAN R M, SURI P, PARK S J. Review: Liquid phase sintering [J]. Journal of Materials Science, 2009, 44: 1−39.

[27] NASH P. The Cr−Ni (chromium−nickel) system [J]. Bulletin of Alloy Phase Diagrams, 1986, 7: 466−476.

[28] ARYA A, BANERJEE S, DAS G P, DASGUPTA I, SAHA-DASGUPTA T, MOOKERJEE A. A first-principles thermodynamic approach to ordering in Ni−Mo alloys [J]. Acta Materialia, 2001, 49: 3575−3587.

[29] LEONHARDT M, LOSER W, LINDENKREUZ H G. Solidification kinetics and phase formation of undercooled eutectic Ni−Nb melts [J]. Acta Materialia, 1999, 47: 2961−2968.

[30] DEMÉTRIO K B, KLEIN A N, SCHAEFFER L, CONSONI D R, MARTINELLI A E, BENDO T. Sinterability and microstructure evolution during sintering of ferrous powder mixtures [J]. Journal of Materials Research, 2013, 16: 1030−1038.

[31] REED R C. The physical metallurgy of nickel and its alloys [C]//The Superalloys: Fundamentals and Applications. Cambridge, UK: Cambridge University Press, 2006: 33−120.

[32] STOLOFF N S. Properties and Selection: Irons, steels, and high performance alloys [M]. Materials Park, OH: ASM International, 2005: 1478−1527.

[33] MOSTAFAEI A, STEVENS E L, HUGHES E T, BIERY S D, HILLA C, CHMIELUS M. Powder bed binder jet printed alloy 625: Densification, microstructure and mechanical properties [J]. Materials and Design, 2016, 108: 126−135.

[34] ÖZGÜN Ö, GÜLSOY H Ö, YILMAZ R, FINDIK F. Injection molding of nickel based 625 superalloy: Sintering, heat treatment, microstructure and mechanical properties [J]. Journal of Alloys and Compounds, 2013, 546: 192–207.

[35] UNVER I, GULSOY H O, AYDEMIR B. Ni-625 superalloy foam processed by powder space-holder technique [J]. Journal of Materials Engineering and Performance, 2013, 22: 3735−3741.

[36] HARGATHER C Z, SHANG S L, LIU Z K. A comprehensive first-principles study of solute elements in dilute Ni alloys: Diffusion coefficients and their implications to tailor creep rate [J]. Acta Materialia, 2018, 157: 126−141.

[37] CIESLAK M J, HEADLEY T J, ROMIG A D, KOLLIE T. A melting and solidification study of alloy 625 [J]. Metallurgical Transactions A, 1988, 19: 2319–2331.

[38] FLOREEN S, FUCHS G E, YANG W J. The metallurgy of alloy 625 [C]//Superalloys 718, 625, 706 and Various Derivatives. Warrendale, PA: The Minerals, Metals & Materials Society, 1994: 13–37.

[39] SMORYGO O, MIKUTSKI V, LEONOV A, MARUKOVICH A, VIALIUHA Y. Nickel foams with oxidation-resistant coatings formed by combustion synthesis [J]. Scripta Materialia, 2008, 58: 910−913.

[40] ASHBY M F. The properties of foams and lattices [J]. Philosophical Transactions of the Royal Society A, 2006, 364: 15−30.

[41] GAO Shuang, HOU Jie-shan, GUO Yong-an, ZHOU Lan-zhang. Phase precipitation behavior and tensile properties of as-cast Ni-based superalloy during heat treatment [J]. Transactions of Nonferrous Metals Society of China, 2018, 28: 1735−1744.

[42] ÖZGÜN Ö, YILMAZ R, GÜLSOY H Ö, FINDIK F. The effect of aging treatment on the fracture toughness and impact strength of injection moulded Ni-625 superalloy parts [J]. Materials Characterization, 2015, 108: 8−15.

提高悬浮浸渍开孔泡沫 Inconel 625 高温合金的烧结动力学和成分均匀性

Oleg SMORYGO[1], Vitali MIKUTSKI[1], Anastasia VAZHNOVA[1], Viachaslau HANCHAROU[1], Serguei TIKHOV[2], Vinod Kumar JANAGAM[3], Amol Anant GOKHALE[4]

1. O.V. Roman Powder Metallurgy Institute, 41, Platonov str., Minsk 220005, Belarus;
2. Boreskov Institute of Catalysis, Siberian Branch, Russian Academy of Sciences, 5, pr. Lavrentieva, Novosibirsk 630090, Russia;
3. Defence Metallurgical Research Laboratory, Kanchanbagh, Hyderabad 500058, India;
4. Indian Institute of Technology Bombay, Powai, Mumbai 400076, India

摘　要：采用悬浮液浸渍法制备开孔泡沫 Inconel 625 高温合金，先用混合粉末悬浮液复制纯镍泡沫带，然后进行热处理。本研究的目的是寻找一种合适的方法，在不使用低熔点添加剂的情况下，确保泡沫高温合金带的完全致密化，并在适中的烧结温度下获得均匀的化学成分。通过扫描电子显微镜和能谱仪对上述方法制备的泡沫带的显微组织和成分变化进行表征，并对其准静态压缩性能进行评估。结果表明，用 Cr、Mo 和 Ni 元素粉末作为高温合金粉末悬浮液的添加剂，在适中的烧结温度下，可获得化学成分均匀、密度高、符合 Inconel 625 标准的高温合金粉末悬浮液。这是因为低熔点共晶的形成，以及存在元素粉末时大的成分梯度所产生的非平衡热力学条件加速了扩散动力学。

关键词：高温泡沫合金；悬浮液复制；烧结；扩散；显微组织

(Edited by Wei-ping CHEN)